The Promotion Effect of Platinum on Gold's Reactivity: A High Resolution Photoelectron Spectroscopy Study

*†*Mauricio J. Prieto,* ‡*Emilia A. Carbonio, Richard Landers and Abner de Siervo*

Departamento de Física Aplicada, Instituto de Física Gleb Wataghin, Universidade Estadual de Campinas, 13083-859, Campinas, SP, Brazil.

Keywords: Platinum, gold, model system, catalysis, alloying.

ABSTRACT: The reactivity of the Pt/Au(332) surface was studied using high resolution photoelectron spectroscopy and carbon monoxide adsorption at 3.5 x 10^{-3} mbar. The characterization of Pt/Au(332) indicates the formation of a Au-Pt surface alloy at the top most atomic layer of the (332) crystal due to an atomic exchange mechanism at both terrace and step edge. The amount of alloyed Au atoms has proven to be dependent on the amount of Pt deposited in the coverage range investigated. The activation of Au atoms by alloying is detected by comparing the ability of the surface to adsorb CO at high pressures. By analyzing the C 1s and O 1s photoemission lines it is possible to conclude that CO adsorption is both dissociative and molecular on the PtAu/Au(332) surface, differently from the behavior observed for Au and Pt single crystals. Also, by rising the temperature of the COads-PtAu/Au(332) surface, a dissociative reaction path is followed with the accumulation of graphitic carbon on the surface and the oxygen desorption. Thus, our results shows, not only the differential catalytic behavior of Pt@Au/Au(hkl) model surfaces but also that Au atoms have an active role on the reaction mechanism.

INTRODUCTION

Transition metal nanoparticles have been extensively studied over the years because of their remarkable properties as catalyst in a variety of materials [1]. These materials have been tested, in some cases successfully, for a wide variety of chemical reactions ranging from dehydrogenation to oxidation of small organic compounds.

Particularly in the case of Pt-based binary nanoparticles, their applicability in the field of electrocatalysis has been a subject of research for the last decades due to the promising results for fuel cell applications. In this sense, the main reactions for which these catalysts have been tested are mainly oxygen reduction[2] and hydrogen[3], methanol[4], ethanol[5] or glycerol[6] oxidation. Whether the material is used as an anode or cathode in a fuel cell, the main concern is the high Pt content of these materials. In order to improve Pt utilization, the so called core-shell nanoparticles were created using different methods where a non-noble metal core is protected by a Au shell where Pt or mixed Pt-TM (TM= transition metal) monolayers are deposited as the main catalytically active phase. In this respect, promising results were reported in the literature for various reactions regarding their application to fuel cells, such as methanol[4, 7-8] and ethanol[8] oxidation, and oxygen reduction [9].

In a general way, the aim of alloying Pt with a second TM is to increase the reactivity of Pt. The mechanism responsible for the activity enhancement is always referred as being due to: i) electronic/ligand or ii) geometric/ensemble effects; although in most cases it is the result of a combination of these effects. In the specific case of the Pt-Au bimetallic system, the effect of Au on the properties of Pt has been rationalized as being a consequence of the lattice mismatch of ca. 4 % between Au and Pt and the possibility of charge transfer from Au atoms to Pt, despite the fact that Au has a higher electronegativity. In this sense, various reports have addressed the enhancement of Pt reactivity due to Au alloying in terms in the case of carbon monoxide [10-11]. However, the role of Au atoms in Pt-Au alloys has been greatly ignored in terms of their participation in the reaction mechanism of the catalyzed chemical or even electrochemical reactions. In other words, the role of Au on Pt@Au alloys, from nanoparticles to thin films, is interpreted as being an indirect modification of Pt of the enhancement of adsorbate-Pt bond strength properties due to electronic and ensemble effect, disregarding the possibility of a direct participation of Au atoms during the reaction.

The adsorption of carbon monoxide (CO) on single crystalline surfaces of Au, both basal and vicinal, has been the subject of many studies in the last decades using a variety of techniques such as TPD, HR-XPS

and FTIR[12-14]. All these papers have reported the weak interaction of CO molecules with Au, reflected by the necessity of performing the adsorption experiment at low temperatures, and supported by simulations [15]. Moreover, increase in the energy of adsorption of CO has been observed, in going from a basal plane to a vicinal surface of Au, indicating the higher reactivity of kink- and step-like surface atoms. Nevertheless, no results on CO dissociation have been reported on Au surfaces, even those having high density of defects, at room temperature.

Accordingly, we propose the use of a Pt/Au(332) substrate as a model surface to study the fundamental properties (electronic and morphological) of Pt@Au core-shell nanoparticles. The morphology of the Pt/Au(332) surface was studied and recently reported in a previous paper[16]. In that report we showed that the growth of Pt nanostructures proceeds via an island formation mechanism. The growth is anisotropic, with the preferential axis of growth being parallel to the step edge due to the energy barrier for hetero-diffusion across the step edge (Ehrlich- Schwoebel barrier). The transition from a monolayer to a bilayer regime was also observed as coverage dependent.

In the present paper we show high resolution photoelectron spectroscopy results that suggest that Pt atoms have a promotion effect on Au atoms by turning them into active sites upon alloying by means of carbon monoxide adsorption/reaction, in contrast to the unmodified Au(332) surface. In this sense, the Pt/Au(332) surface exhibit a unique catalytic behavior for CO cracking at room temperature, differently from Au and Pt bare surfaces both basal and vicinal. Additionally, the results suggest that Au atoms may have an active role in the adsorption/reaction of CO in addition to the indirect modification of the catalytic properties of Pt nanostructures since a different catalytic response was observed compared to both bare Pt and Au surfaces.

RESULTS AND DISCUSSIONS

Bare Au (332) surface: characterization and reactivity

Prior to the deposition of Pt nanostructures, the Au(332) surface is characterized. The results of high resolution core level (HRCL) spectra before and after CO exposure are shown in Figure 1 and the fitting results are presented in Table S1 available in the Supplementary Electronic Material.

In the case of clean Au(332) the fitting procedure reveal the existence of 2 components in the Au $4f_{7/2}$ core line. As can be seen from the data in Table S1, a splitting of -0.33 eV is obtained for the surface component relative to the sub-surface feature. This value is in excellent agreement with data already published for surface core level shifts on basal planes of Au [17]. Also, the intensity ratio (surface/sub-surface)

calculated from peak's area is in agreement with the expected value for a probing depth of 2 atomic layers (hν = 180 eV). From now on, the components will be referred to as surface and sub-surface. At this point it is worth mentioning that, according to data reported in the literature for the inelastic mean free path of Au 4f photoelectrons with a kinetic energy of 95 eV [18] and the intensity ratio of the components shown in spectra of Figure 1a (surface:sub-surface = 1.2) we conclude that, under the experimental condition used, the signal should be limited essentially to the surface and sub-surface atomic layer of the Au(332) crystal.

In order to investigate the reactivity of the bare Au(332) substrate prior to Pt deposition the surface was exposed to CO and HRCL spectra were collected after the exposure. The resulting Au $4f_{7/2}$ spectra are shown in Figure 1b and the parameters resulting from the fitting are presented in Table S1. Fitting results reveal that no changes are observed on the Au $4f_{7/2}$ photoemission line in terms of chemical shifts of the surface feature or even intensity ratio of the two components considered in the fitting. The presence of C is detected after exposure to CO but at a very low concentration as can be inferred from the comparison of C1s spectra for the Pt/Au surface, as discussed in the next section (see Figure 7, red line). In contrast, no O is detected on the surface under the experimental conditions used. Considering the fact that the atomic subshell photoemission cross section of C 1s and O 1s lines are comparable at the photon energies used (400 and 650 eV, respectively)[19], one could expect the same sensitivity for detection of C and O, implying that only C is indeed present on the surface after exposure. This result and the BE of this feature suggest that C detected should be a CH_x specie rather than CO, a common contaminant of even high purity CO gas that becomes significant when working at relatively high pressures. However, since its surface concentration is very low, its presence does not change the results that will be shown in the next section regarding the adsorption studies on Pt/Au(332).

The adsorption of CO on bare Au single crystals of low Miller index such as (111), (100) and (110) has been explored in the past by various authors [20-22]. Even though these results were obtained by adsorbing CO at low temperatures, they provide an interesting framework to understand the reactiveness of Au surfaces. Also, among the three basal planes, the (110) plane can be considered as being part of the same family of planes as Au(332), having the structure Au(S)[n(111)x(111)], with n indicating the number of atoms that constitute the terrace and the 3 numbers in parenthesis the crystallographic orientation of the terrace and the step, respectively. In the case of Au(332), n = 6, while in the case of Au(110) n = 2. Because of this, the (110) surface is a suitable candidate for comparison in terms of reactivity, since it has the maximum density of step-like defect possible for this vicinal family. In this sense, Meier et al. [21] reported that for a Au (110) surface, for temperatures above 250 K, the adsorption of CO is discarded for

by means of infrared reflection absorption spectroscopy data at pressures in the mbar range. These results agree very well with the absence of adsorbed CO on Au(332) observed from HRCL spectra of Figure 1b. The role of under-coordinated atoms in the adsorptive properties of Au surfaces has been discussed by Mehmood et al. [20] and the calculated energy of adsorption of CO on flat, stepped and kinked Au reveals a stronger adsorption on under-coordinated atoms; although, the energies of adsorption obtained are considerably smaller than for Pt surfaces. Weststrate[12] and Ruggiero[13] obtained the same conclusion using vicinal surfaces as substrates and techniques such as high resolution XPS, TPD and FTIR spectroscopy.

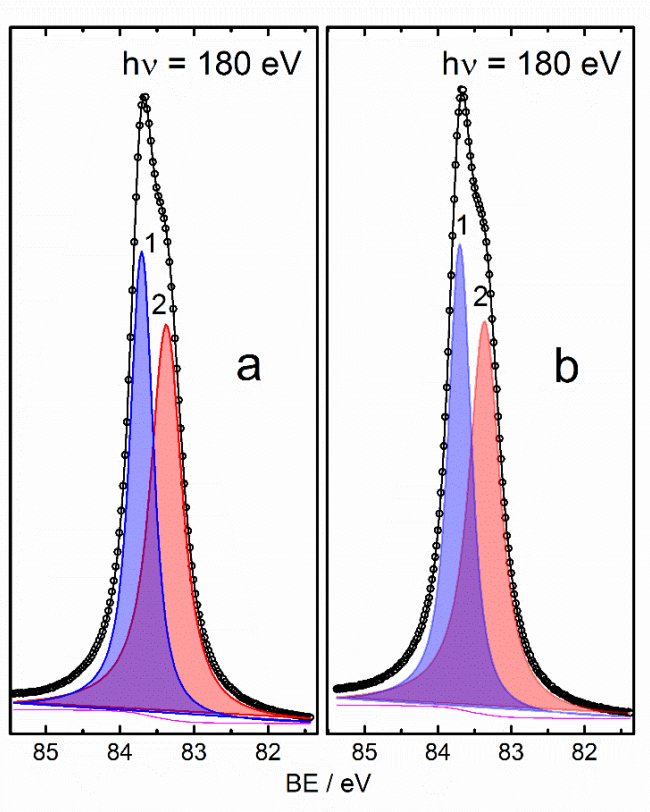

Figure 1. High resolution spectra of $4f_{7/2}$ core line for Au(332) taken before (a) and after (b) exposure to CO at room temperature. CO dosing was 7.9 x 10^6 L. Red (2) and blue (1) components represent surface and sub-surface contributions in both cases, respectively.

From all the arguments presented above we believe that CO adsorption must be reversible on Au(332), i.e., CO molecules physically adsorbs onto Au(332) surface but once CO is pumped out of the UHV chamber, the adsorbed molecules desorb, leaving behind a bare Au(332) surface. Moreover, the adsorption should be molecular, since no measurable traces of graphitic carbon were detected in our experiments with the bare Au(332) surface. This is an important result since the modification with Pt induces a different behavior from the catalytic point of view, as will be discussed in the next section.

The effect of adding Pt on Au(332)

Figure 2 shows the high resolution core level spectra of Au $4f_{7/2}$ and Pt 4f photoemission lines for a sample having a Pt/Au ratio of 0.136 (all peaks were normalized for the corresponding photoemission cross-section and analyzer transmission). As can be seen, in the case of Au, the existence of a third component at the lower BE tail of the $4f_{7/2}$ line emerges after Pt deposition (green component (3) in Fig. 2a at 83.20 eV). The position of this third component does not change with surface concentration of Pt, although its contribution to the total envelope increases almost linearly with Pt/Au ratio, thus confirming its assignment to Au atoms in close contact with Pt atoms, as shown in Figure 3. The Au surface component belonging to Au atoms in the vicinity of Pt ad-atoms (component 3) shows a chemical shift of ca. -0.21 eV relative to the bare surface (component 2), leaving the position of sub-surface and "pure"-surface components (1 and 2) unchanged. Moreover, regarding the Pt $4f_{7/2}$ photoemission line in Figure 2b, the presence of a main component is detected at ~70.1 eV (component 1), representing a negative shift of ca. -0.8 eV compared to the value reported by Keister et al.[23] for Pt nanostructures on SiO_2 (see red line in Figure 2b), where no strong Pt-support interaction is expected.

The results obtained from the fitting of both Au and Pt $4f_{7/2}$ lines for various samples are presented in Figure S1 in the Electronic Supplementary Material. For instance, in all samples three components were detected for Pt (see numbers in Fig. 2b), in contrast to Au where only one additional component under Au $4f_{7/2}$ line emerges upon deposition (component 3 in Fig. 2a). In the case of Pt, results suggests that as the coverage increases, at least two different types of Pt emerge having both components 1 and 2 a BE lower than that expected for bare Pt. From the fitting results it is observed that the component at 69.80 eV (component 2) increases with Pt coverage in detriment of the main component at 70.08 eV (component 1), a trend that is depicted in Figure 3. This behaviour arises from the fact that as coverage increases there

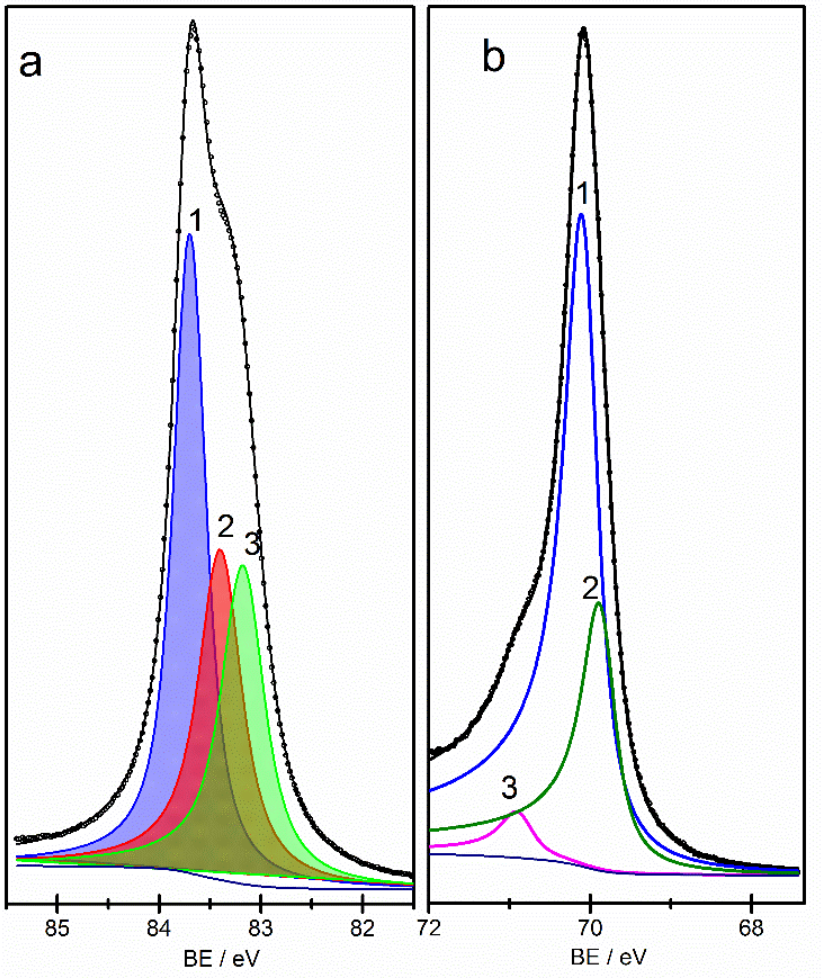

Figure 2. High resolution core level spectra recorded at room temperature and fitting results of Au $4f_{7/2}$ (a) and Pt $4f_{7/2}$ (b) photoemission lines for the sample with Pt:Au ratio of 0.136. Components 1, 2 and 3 under the Au 4f7/2 line correspond to subsurface, surface and surface alloyed gold contributions, respectively. Components 1,2 and 3 under Pt 4f7/2 line correspond to 1st and 2nd layers on Pt nanoislands and impurity, respectively. For results regarding samples having a different Pt:Au ratio the reader is referred to the Supplementary Electronic Material of this manuscript available online.

is a transition from monolayer (ML) to bilayer (BL) heights of the nanoislands, as demonstrated by us in a previous report using scanning tunnelling microscopy[16]. Thus, component 2 could be ascribed to the topmost atomic layer of bi-layered nanoislands, with the atomic layer beneath being responsible for component 1. Thus, both components show a negative shift compared to a bare Pt surface due to the tensile strain by the lattice mismatch between Au and Pt, but component 2 appears at even lower BEs in the same way that the surface-core level shift emerges in $4f_{7/2}$ photoemission line of clean gold (component 2 in Fig. 1a). Furthermore, component 3 (at ca. 71 eV) could be explained by the contamination at a very low extent of the very reactive Pt ensembles during the experiment.

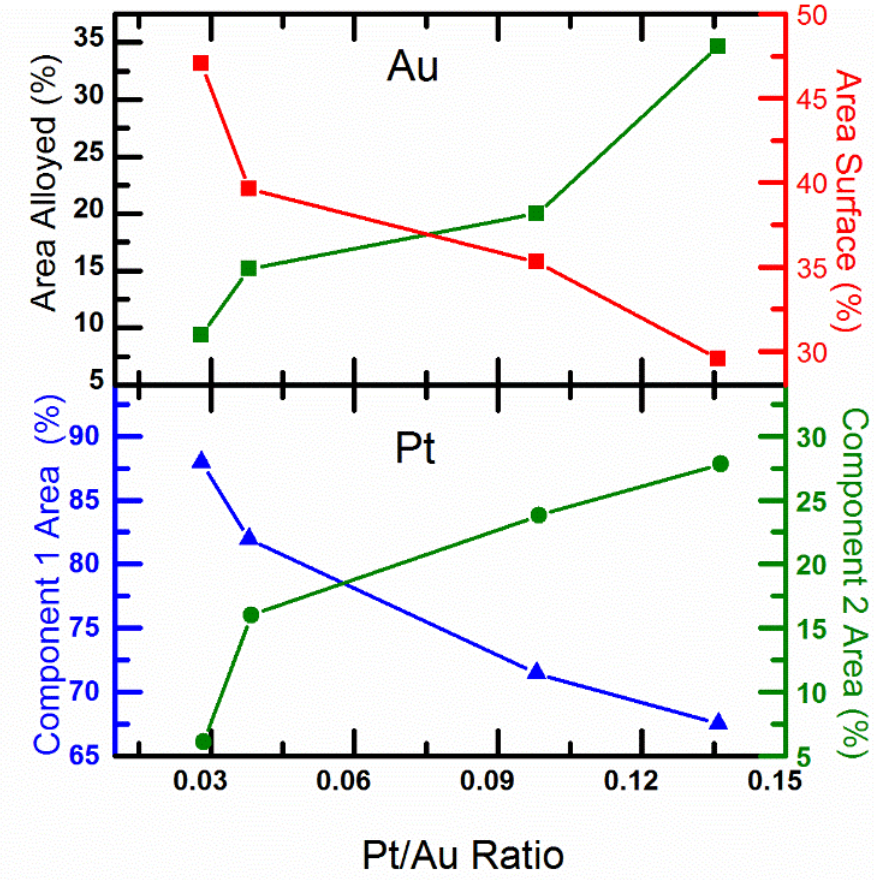

Figure 3. Variation of components area under Au and Pt $4f_{7/2}$ core lines extracted from fitting of spectra in Figure S1 of the Electronic Supplementary Material for Pt/Au(332) samples with different Pt:Au ratios. Green and red curves in the upper graph correspond to alloyed and surface contribution in Au 4f line, respectively. Blue and green curves in the lower graph correspond to the contributions from 1st and 2nd atomic layer in Pt nanoislands.

The fact that, for both Pt and Au, a negative shift is observed upon deposition indicates the existence of an atomic exchange process between Au and Pt atoms at the topmost atomic layer of Au(332) at room temperature, since similar chemical shifts have been reported for Pt-Au bulk alloys by Hörnström et al. [24], with the magnitude of the chemical shift being dependent of the alloy composition for both surface and bulk Au and Pt core levels. Some papers, as for example in ref.[11], have addressed the possibility of an interatomic exchange in the first layer of Au(111) upon Pt deposition, especially in the low coverage limit, suggesting that the formation of a phase of mixed composition is plausible.

We showed in a previous publication that Pt grows on the Au(332) surface via island formation with a monolayered (ML) to bi-layered (BL) phase transition upon deposition, within the coverage range investigated. The growth proceeds anisotropically with the preferred axis of growth being parallel to the step-

edge, since the surface diffusion across the monoatomic step is hindered at room temperature due to the Ehrlich-Schwoebel barrier. In this sense, these new results regarding the HR-XPS study corroborates that the nanoislands should have mixed composition generated by the atomic exchange of topmost Au atoms of the Au(332) surface with incoming Pt. In this context, the negative shifts observed in Pt 4f line (see Fig. S2 in electronic supplementary information) can be attributed to the fact that Pt atoms inserted into the Au matrix are submitted to tensile strain due to the lattice mismatch between Au and Pt. In the case of Au, a d-band shift of the occupied d-states has been predicted by Freire et al.[25] for the Pt/Au(111) surface, within the intermixing scenario, using DFT calculations (ca. 0.2-0.4 eV depending on the surface composition). In this sense, the direction and magnitude or the d-band center shift correlates the chemical shifts for the alloyed Au component. We believe that this comparison is valid since the Au(332) surface contains (111) domains (terraces) separated by monoatomic steps. Thus, our results strongly suggest that in the case of Pt/Au system both electronic and ligand/geometric effects are important in determining the final properties of the model Pt/Au(332) surface.

Many authors have discussed the driving force for Pt-Au intermixing in the Pt/Au(hkl) and Au/Pt(hkl) systems. For instance, Stolbov et al.[26] calculated the Pt-Pt and Pt-Au binding energy and concluded that Pt-Pt interaction is stronger than Pt-Au, something that could be related with a segregation trend. However, Bergbreiter et al.[27] showed that the entropic factor due to dilution is a very important aspect that cannot be disregarded and ultimately may lead to the formation of a surface alloy. Still, the extent of miscibility of both metals will ultimately depend on the temperature of the sample, provided that atom mobility is sufficient to allow inter-diffusion.

Figure 4 shows a sphere model of the Pt/Au(332) surface structure with different scenarios that may arise upon Pt deposition on Au(332) depending on the Pt surface loading. For instance, at very low coverage, the incoming Pt atoms can be exchanged with Au atoms both in the terrace and at the step edge, with the more favorable position being the step edge position due to the uncoordinated nature of these type of atoms, as we were able to corroborate with STM [16]. Thus, the displaced Au atoms begin to form 2D agglomerates where new Pt atoms can condense, forming nanoislands of mixed composition. As coverage increases, nanoislands undergo a ML to BL phase transition, with the first layer having a mixed composition. The different chemical environment of these Au atoms is responsible for the third component in HR-XP spectra in Figure 2a (green component). The fact that this component exhibits appreciable changes upon CO adsorption on both Pt and Au 4f core lines in the HR-XPS spectra is a strong indicative that both sites, Pt and Au, are involved in the adsorption/reaction. For instance, the adsorption of CO molecules on Au sites in surfaces having Pt-Au mixed sites has been predicted by Ge[28] and Tereshchuk et al. [15] using

Density Functional Theory (DFT). The authors' explanation for this behavior is that the d-band center of Au in a PtAu alloys shifts upwards towards the Fermi level, giving rise to a strengthened CO-Au bond. In this sense, the same behavior is expected for Pt where the same shift in d-band center is observed. Experimental evidence of the stronger CO-Pt chemical bond in this system was reported by Prieto and Tremiliosi-Filho [10] where the onset potential for CO electrooxidation has proven to be higher than for bare Pt on a series of Pt/Au(hkl) electrodes belonging to the same family of planes.

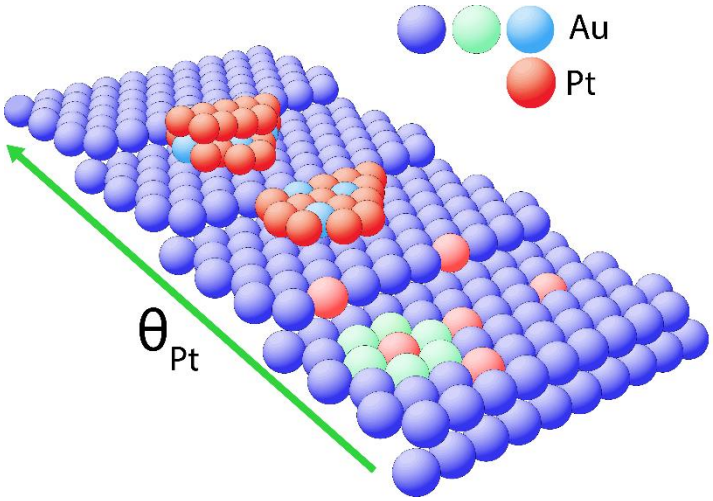

Figure 6. Sphere model of the Pt/Au(332) surface showing the origin of the components observed in high-resolution core level spectra of Figure 3. The scheme represents the different situations that can be found on the crystal surface depending on the amount of Pt deposited. Red spheres represent Pt ad-atoms that can be incorporated into the Au matrix or form nanoislands on the surface of the crystal. Green and light-blue spheres represent Au atoms either in the surrounding of an inserted Pt atom or within a nanoisland, respectively.

Reactivity of Pt@Au/Au(332)

Figure 5 shows a set of normalized high resolution spectra for two samples having different Pt:Au ratio before and after exposition to 7.9 x 10^6 L of carbon monoxide. As can be seen, a series of changes can be ascribed to the specific adsorption of CO, differently from the behavior observed for the bare Au(332) exposed to CO. For instance, a completely new feature in Pt 4f appears after adsorption, indicating the existence of a new chemical state of Pt atoms. The centroid of this new signal is shifted from the main Pt component by +1.2 eV, indicating that the new feature originated upon CO adsorption does not match the BEs reported for platinum oxides (PtO_x), with a chemical shift higher than +1.8 eV [29], depending on the chemical nature of the oxide. Regarding the line shape of Pt 4f lines, Tao et al.[30] reported a similar change for CO adsorption on vicinal Pt(557) surface under similar experimental conditions. In their case, the

authors suggested that the adsorption should be reversible, inducing structural changes in the stepped structure of the surface by breaking the stepped nature of the clean surface. However, the authors discarded the possibility of a dissociative adsorption path, even at relatively high pressures.

On the other hand, the changes observed in Au $4f_{7/2}$ photoemission line in Figure 5 are interesting in the sense that they depict the promotion effect that Pt has on Au due to the surface exchange process. For instance, it is possible to see that the adsorption of CO promotes a chemical shift of the alloyed component at lower BEs on both samples of +0.1 eV (see blue and red arrows in the figure). Chemical shifts in the same direction have been reported by other authors regarding the adsorption of CO at low temperatures on a series of vicinal Au surfaces[12-13], where the new component on Au photoemission line emerges at temperatures below 100 K, although the magnitude of the chemical shift is significantly higher. At this point it is important to emphasize that all data reported in the literature regarding the study of the interaction of bare Au surfaces, basal or vicinal, have been performed at low temperatures and, as it is well known, bare Au weakly interacts with gases at room temperature. In this respect, CO adsorption experiments performed on bare Au(332) under the same experimental conditions did not show the changes in Au $4f_{7/2}$ core line as in Figs. 5 a and b, thus confirming the apparent lack of reactivity of the unmodified surface despite the high density of steps.

In both samples studied, the high resolution spectra of C 1s photoemission line indicates the existence of two different features in the C 1s region. Based on studies of carbonaceous species on Au, the contribution at 283.97 eV could be associated with graphite-like carbon[31] resulting from the dissociative adsorption of CO on Pt@Au mixed sites. Moreover, the component at 286.4 eV can be associated with CO following a molecular adsorption. It is worth mentioning that O 1s line is also detected, supporting our assignment to the aforementioned component at BE > 286 eV. Thus, the C 1s component with higher BE is in agreement with data reported by various authors for the adsorption of CO on a series of TM(hkl) surfaces[32-35].

A more detailed analysis of HR XPS spectra was performed for the sample with Pt:Au = 0.136 and the fitting results of Pt, C and O lines are presented in Figure 5. Parameters extracted from the fitting can be found in Table 1. The main conclusion drawn from these results is that the C feature at higher BE is composed by 3 components at 288.10, 287.11 and 286.43 eV. These components, when compared with data reported in the literature, can be ascribed to C belonging to CO adsorbed on Pt in top and bridge positions (287.11 and 286.43 eV)[36] and on Au (288.10eV)[12, 14], once again suggesting that both Pt and Au sites are active for CO adsorption at room temperature; the same contributions of top and bridge positions

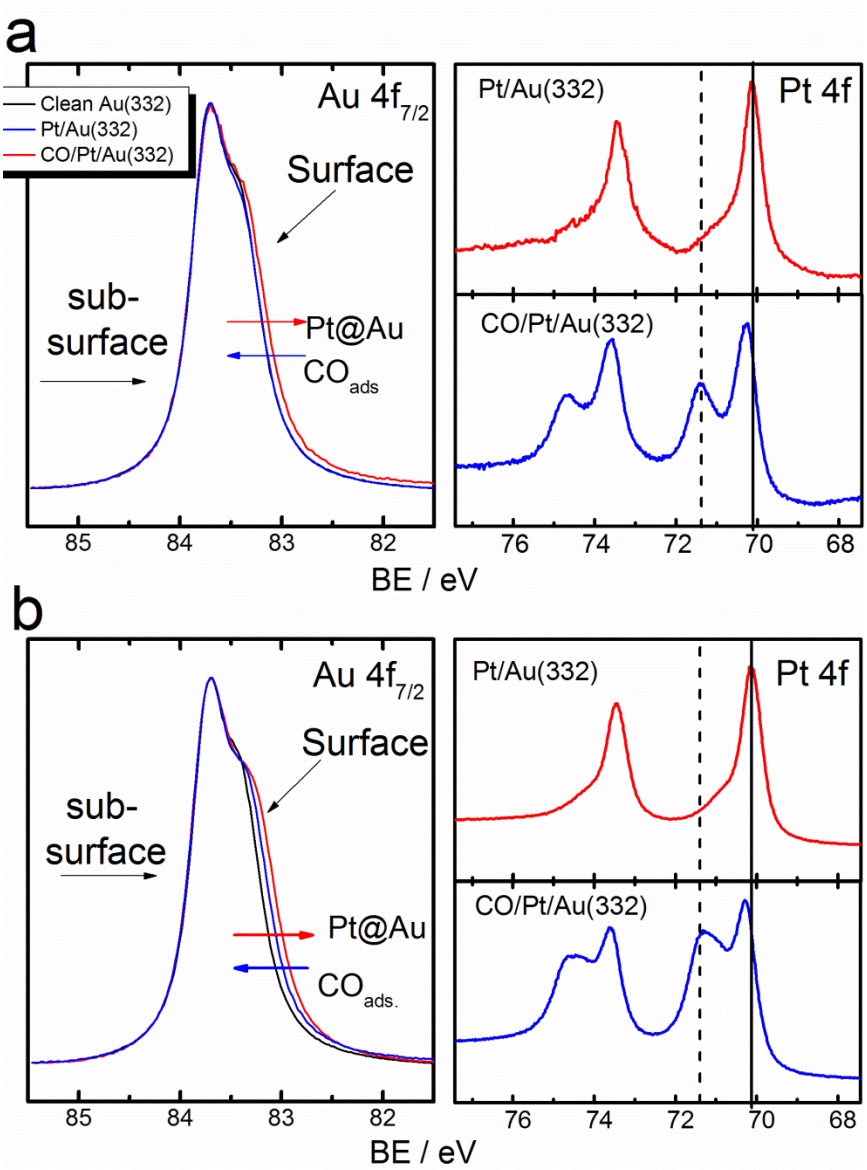

Figure 5. High resolution core level spectra of Au 4 $f_{7/2}$ and Pt 4f photoemission lines, as indicated, for two different samples. Pt/Au ratio of 0.028 (a) and 0.136 (b). Carbon monoxide dosing was done at room temperature and with an exposure of 7.9 x 10^6 L. All spectra were collected with a photon energy of 180 eV.

are detected in O 1s core line (with the BE range in agreement with data already reported[30]). It is worth mentioning at this point that the assignment of the C 1s component at 288.1 eV is in agreement with the results of Eyrich et al.[11] regarding TPD studies of CO on PtAu/Pt(111) surfaces and those reported by Tereshchuk et al.[15] predicted by DFT simulations for the Pt/Au(332) system. However, since the surface

has a mixed composition due to the interatomic exchange of Au and Pt atoms, we believe that bridge sites could be both homogeneous and heterogeneous; i.e., formed by Pt-Pt or Pt-Au atoms. Moreover, the low intensity (area) of the Au-CO component under the C 1s line can be explained by the fact that only those Au atoms that are surrounded or in the vicinity of Pt atoms have their adsorptive properties modified by geometric/electronic effect. Furthermore, we estimate an equivalent coverage for the sample with Pt:Au = 0.136 of 0.27 ML, meaning that only a small fraction of the total amount of Au surface atoms are indeed tune by the presence of Pt. Fitting results of the Pt $4f_{7/2}$ core line reveal the existence of 2 different components, other than the main metallic component, under the new feature that arises upon CO adsorption at 71.00 eV and 71.43 eV. We believe that these components can be ascribed to CO molecules bounded to Pt atoms at two different Pt sites, in agreement with the two CO-Pt components observed under C 1s photoemission core line; the component at higher BE being a contribution of "pure" Pt-Pt sites and Pt sites surrounded by Au atoms. It is possible to see that the contribution to the total envelope of component 2 in Figure 6 decreases after CO exposure, thus indicating that CO adsorption is taking place at the topmost Pt atomic layer of the nanoislands.

The dissociative adsorption CO on pure Pt(hkl) surfaces, both basal and vicinal, has been reported by McCrea et al.[37]. The authors determined that the existence of under coordinated atoms have the ability to break the C–O bond at pressures in the mbar range even on Pt(111). However, they reported that a critical temperature is needed in order to promote the cracking of the pre-adsorbed molecule, the temperature being dependent on the density of defects on the surface. On the other hand, results regarding CO adsorption on stepped Pt(hkl) surfaces indicate that the process is molecular rather than dissociative[38]. In this sense, our results indicate that the Pt@Au/Au(332) surface has an inherent ability for the dissociation of CO since this process is observed at room temperature.

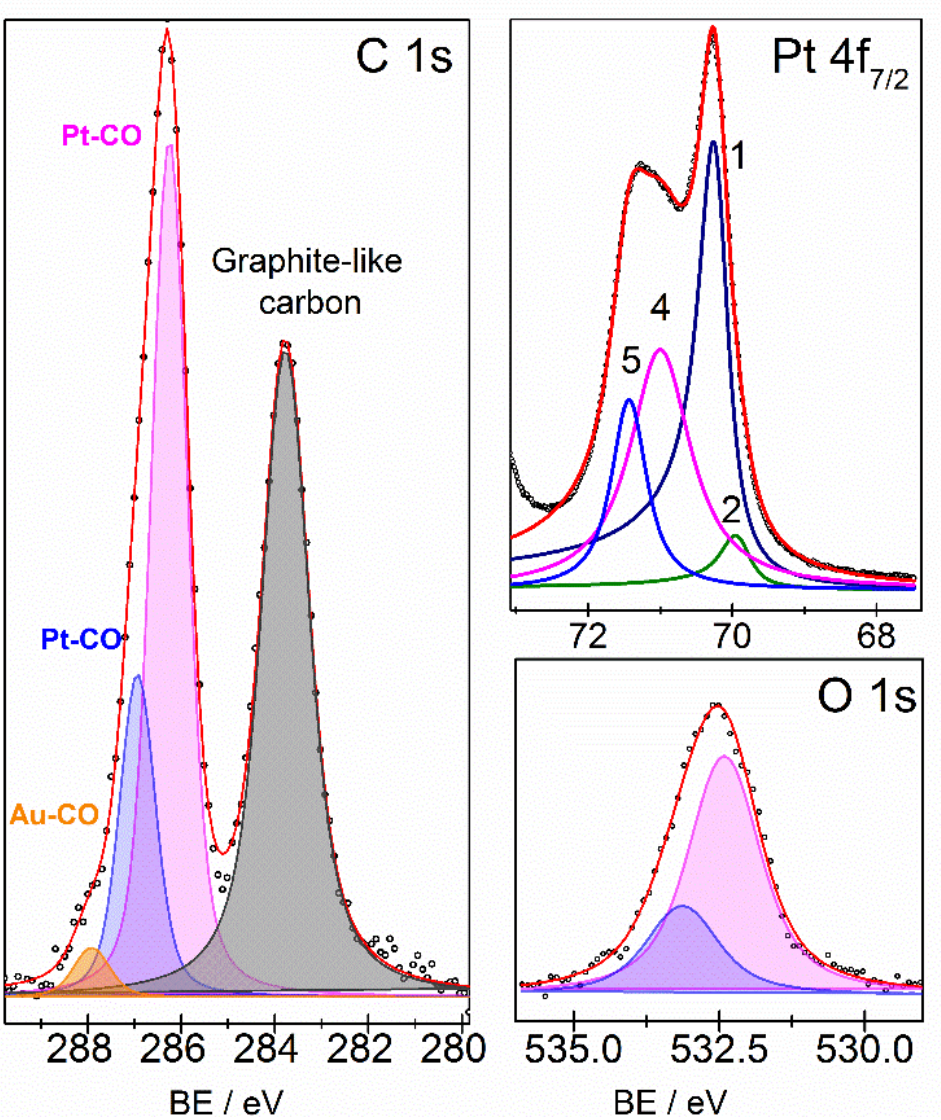

Figure 5. High resolution spectra and fitting results for C 1s, Pt $4f_{7/2}$ and O 1s photoemission lines corresponding to the CO/Pt/Au(332) sample having a Pt:Au ratio of 0.136. All spectra were recorded at room temperature and after CO dosage of 7.9 x 10^6 L. Contribution of Pt-CO in bridge and on-top position can be seen under the C s1 line, in addition to CO-Au and graphitic carbon, resulting from the cracking of CO. For Pt 4f line, component 1 and 2 correspond to contributions originated from the 1st and 2nd layers on Pt nanoislands and components 4 and 5 to Pt-CO in top and bridge configuration, respectively. Blue and magenta components under O1s line correspond to top and bridge positions, respectively.

In order to study the reactivity of the Pt@Au/Au(332) surface, the sample having a Pt:Au ratio of 0.136 was submitted to thermal annealing after CO exposure, since this sample exhibited the more pronounced

changes in the Au $4f_{7/2}$ core line. Figure 7 shows a set of high resolution spectra for Au $4f_{7/2}$, Pt 4f, C and O 1s photoemission lines before and after the thermal annealing.

A series of changes take place after the annealing. For instance, regarding the Pt 4f lines, the vanishing of the components at higher BEs as the annealing proceeds is evident. In addition, the changes in Au line at the low BE tail are consistent with the promotion of Pt incorporation. For instance, component 3 under Au $4f_{7/2}$ core line shifts to lower BE with annealing indicating that the temperature rise promoted the intermixing of Au and Pt atoms, which is in agreement with the expected antisegregation behavior predicted for Pt/Au(hkl) by Ruban et al.[39] using density functional theory and the STM results reported by Bergbreiter et al. for Au/Pt(111)[27].

On the other hand, the most drastic changes can be observed in the C 1s photoemission line, as can be observed from Figure 7. In this case, HR-XPS spectra suggest that thermal annealing induce a drastic change in the CO-related components under the C 1s line, as evidenced from the variation in the intensity ratio of both carbon signals. For instance, the intensity of graphite-like signal (C2) increases in detriment

Table 1. Parameters resulting from the fitting of photoemission lines presented in Figure 5.

Photoemission line	Component	Binding Energy (eV)
C 1s	CO-Au	288.10
	CO-Pt_{bridge}	287.11
	CO-Pt_{top}	286.43
	Graphite-like	283.97
O1s	CO-Pt	533.13
	CO-Pt	532.41
Pt $4f_{7/2}$	Pt@Au-CO	69.92
	Pt-metallic	70.23
	Pt-CO	71.00
	Pt-CO	71.43

.

of the CO related one (C1), suggesting a transformation of one type of carbon into the other, provided that all spectra were normalized by Au $4f_{7/2}$ intensity and the respective cross sections of C 1s and Au 4f lines. Accordingly, the intensity of O 1s line decreases upon annealing, following the diminution in C1 signal. All these results suggest that the surface is catalytically active for the cracking of the carbon monoxide molecule, leading to carbon that builds up on the surface and, probably, molecular oxygen that desorbs from the surface due to its low affinity with the surface as stated by various authors for bare Au crystals[40-41]. Since the calculated Pt:Au ratio is rather small for the sample submitted to thermal annealing (0.136) we expect that part of the surface should correspond to virtually "pure" unmodified Au, with no Pt atoms in the vicinity, whose local activity may well resemble the activity of bare Au surfaces (unreactive or with low reactivity towards molecular oxygen adsorption). For instance, even with the possibility of oxide formation, it has been demonstrated that Au_xO_y layers are rather unstable and prone to decomposition under UHV, suggesting the existence of a dynamic equilibrium between the oxide layer and oxygen at the gas phase[42].

As a general picture of the surface and its reactivity we offer the following explanation. The atomic exchange process that occurs at the surface as soon as incoming Pt ad-atoms arrive at the Au substrate generates basically two types of adsorption sites for carbon monoxide molecules, in addition to those already present on the unmodified surface (step-edge Au atoms), being Au alloyed and Pt sites. In both cases, the effect of the atomic exchange is a negative shift of the d-band center towards the Fermi level, as can be anticipated[43] from the negative shifts observe in core-line spectra of Au and Pt. As a consequence, a stronger CO-Metal interaction is expected and this was particularly detected in the case of Au, since no changes were observed in the Au $4f_{7/2}$ core line upon CO exposition on bare Au(332) compared to the Pt-modified surface. As a consequence, the adsorption of CO on both Pt and Au sites is detected, since different C 1s signals belonging to different CO-Metal bonds were detected, as already discussed. Also, a dissociative adsorption of CO is observed at room temperature, differently from bare Au and Pt surfaces. In this sense, it seems that this effect is a new property that arises from the alloying process, although molecular adsorption is also detected as in the case of the pure counterparts even in the case of vicinal surface where a high density of uncoordinated atoms is available for the reaction to occur. Therefore, Au sites seem to play an important and active role on the reactivity of the surface, in addition to the indirect modification of the electronic properties of Pt nanostructures by charge transfer or even by a geometric effect due to lattice mismatch.

The extent of ensemble effect on Au/Pt(111) has been the subject of study of various publications [27, 44-45]. In these reports it is demonstrated that the process a surface atomic exchange may induce a modification on the surface atomic distribution that will have a direct impact on the reactivity of the surface as a whole. For instance, the formation of dimers or even trimer structures of Pt modifies the adsorption site preference of CO, something that may ultimately lead to different reaction paths. Although these results are focused on the Au/Pt(111) complementary systems, we believe that the same situation is valid for the Pt/Au(332) reported in the present paper. In this case, we also believe that the geometry of Au ensembles should play a significant role on the reactivity of the surface, besides that of the Pt ensembles.

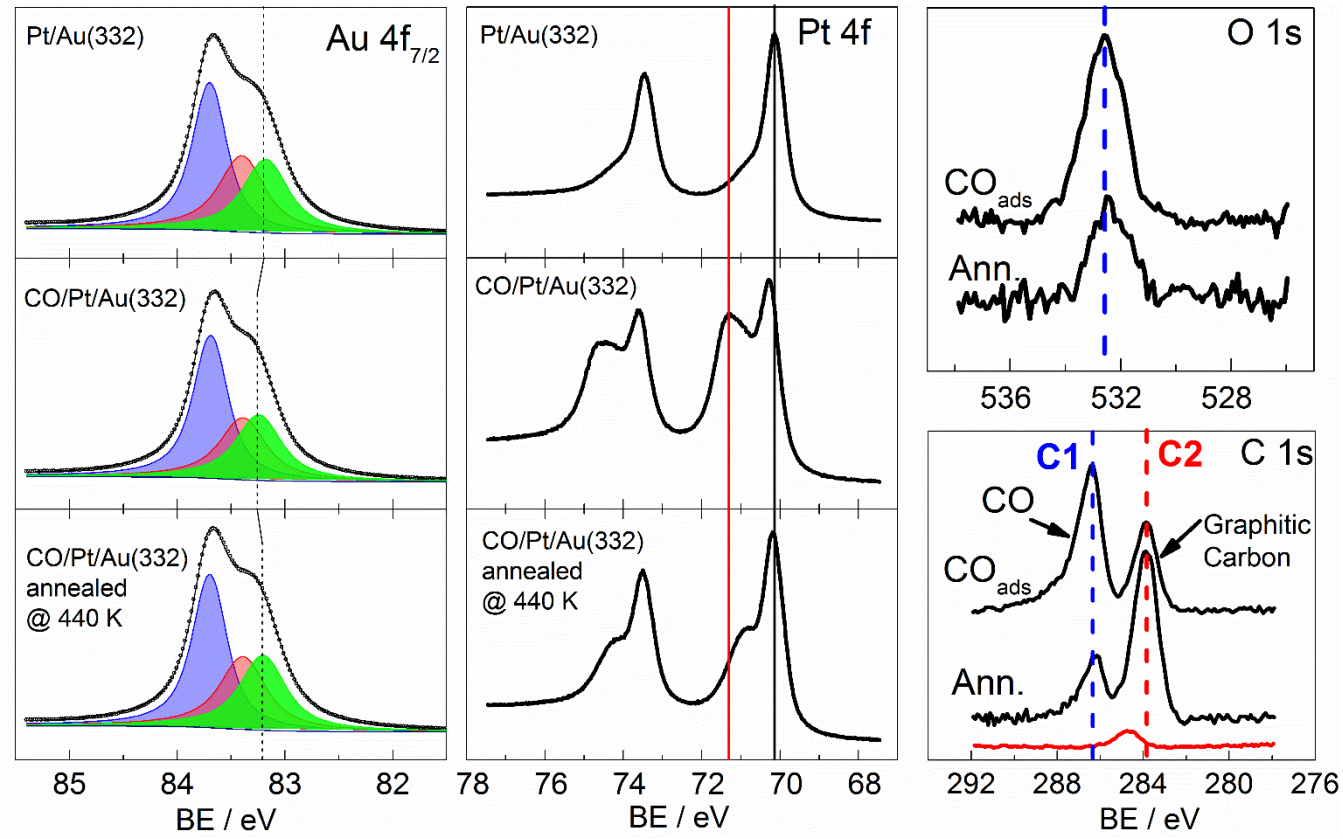

Figure 7. HR-XP spectra showing Au4f$_{7/2}$, Pt 4f, C and O 1s photoemission core lines for the sample with Pt/Au ratio of 0.136 before and after exposition to 7.9 x 10^6 L of CO at room temperature and after annealing at 440 K for 10 minutes, as indicated. Red spectra in C 1s set correspond to feature observed after CO exposure of unmodified Au(332). For fitting results of C 1s, O 1s and Pt 4f$_{7/2}$ lines the reader is reffered to the Electronic Supplementary Material available online.

CONCLUSIONS

The electronic properties of the Pt/Au(332) interface were addressed by means of high resolution photo-electron spectroscopy using synchrotron radiation. The deposition of Pt nanostructures on the vicinal Au surface proceeds following an atomic exchange process at the topmost atomic layer of the Au(332) crystal, at both terrace sites and step-like sites. Consequently, a negative shift of 4f core levels of both Au and Pt is anticipated, towards the Fermi level with the corresponding chemical shift on both 4f core lines in HR-XPS spectra.

We were able to determine that the atomic exchange process has a promotion effect on gold's reactivity by activating the Au atoms initially with a low affinity for CO adsorption/reaction. The CO adsorption on PtAu/Au(332) has proven to be both molecular and dissociative giving rise to graphite-like carbon on the surface in addition to adsorbed CO. The dissociative path seems to be the preferred reaction path at temperatures higher than room temperature, as evidenced by the changes observed in C and O 1s core lines of high resolution spectra. In this sense, the role of Au atoms have proven to be essential for this behavior, since the dissociative adsorption at room temperature has not been reported on single crystalline surfaces (basal or vicinal) of both transition metals.

AUTHOR INFORMATION

Corresponding Author
* Dr. Mauricio J. Prieto.
Email: prietomauricio@gmail.com; prieto@ifi.unicamp.br; prieto@fhi-berlin.mpg.de
Present address:
†Abteilung Chemische Physik, Fritz-Haber Institut der Max-Planck-Gesellschaft, Faradayweg 4-6, 14195 Berlin, Germany.
‡ Helmholtz-Zentrum Berlin für Materialien und Energie, BESSY-II, Albert-Einstein-Straße 15, 12489 Berlin, Germany.
‡Abteilung Anorganische Chemie, Fritz-Haber Institut der Max-Planck-Gesellschaft, Faradayweg 4-6, 14195 Berlin, Germany.

Author Contributions:
The manuscript was written through contributions of all authors. / All authors have given approval to the final version of the manuscript. / All authors contributed equally.

ACKNOWLEDGEMENTS

Authors thank Fundação de Amparo à Pesquisa do Estado de São Paulo (FAPESP-07/54829-5) and Conselho Nacional de Desenvolvimento Científico e Tecnológico (CNPq) for financial support. Specialy

thank to Prof. G. Tremiliosi-Filho for lending the Au(332) crystal. MJP and EAC thank FAPESP and CNPq for the fellowships granted (Proc. FAPESP 2011/12.566-3; Proc. CNPq 150192/2014-2). Authors also thank the Brazilian Synchrotron Light source for the beam time and the PGM-beamline staff for support during the experiments.

ASSOCIATED CONTENT

*Supporting Information

Detailed description of the procedure and lineshapes used for the fitting of high resolution spectra; values of the parameter fitted for Au $4f_{7/2}$ and Pt 4f for clean Au(332) and platinum modified samples.

This material is available free of charge via the Internet at http://pubs.acs.org

EXPERIMENTAL SECTION

All experiments were carried out in an ultra-high vacuum (UHV) system. The chamber is equipped with LEED optics, an Omicron HA 125 hemispherical electron analyser with 5-channeltron detection, an Ar ion gun for sputtering, a water cooled e-beam evaporator and a high precision two rotation axis manipulator, allowing sample transfer and heating up to 1200 K by electron bombardment. The setup operates in a base pressure of 7×10^{-11} mbar and in the 1.2×10^{-10} mbar regime during evaporation and measurements.

Au(332) crystal was purchased from MatecK Gmbh with orientation accuracy better than 0.1°. In order to clean the surface prior to each set of measurements sputtering of the surface was performed at 1 keV for short periods of time, followed by annealing at 730 K for 15-30 minutes in UHV. The surface order was determined by means of Low Energy Electron Diffraction patterns showing the corresponding spot splitting with 3-fold symmetry of the (332) plane.

Pt nanostructures were grown using the e-beam evaporation technique from a 99,995% Pt wire purchased from Alfa-Aesar which was exhaustively outgassed in order to avoid contamination during evaporation. Evaporation flux was kept constant and deposition time was varied in order to reach different coverage. The Au vicinal substrate was kept at room temperature during deposition in order to avoid Pt diffusion into Au matrix. As a measure of the Pt surface concentration, Pt/Au ratios were calculated from data resulting from the fitting and the proper normalization of the corresponding photoionization cross-sections[15]. All XPS measurements were performed at normal incidence and room temperature.

The CO adsorption experiments were performed in a adjoin reaction chamber where exposition to high pressures of 99,99 % CO is allowed. All exposures were made following the same procedure, with 7.9×10^{6} Langmuir (3.5×10^{-3} mbar for 5 min). Thermal annealing of Pt/Au(332) sample previously exposed to CO was performed at 440 K for 10 minutes.

High resolution XPS experiments were performed at the U11 PGM-beamline at the Brazilian Synchrotron Light Source (LNLS). Pt and Au 4f core line spectra were collected using a photon energy of 180 eV, while O and C 1s lines were collected with photon energies of 650 and 400 eV, respectively. The uncertainty in BE determination is estimated as being 0.02 eV according to data reported for this beamline [46]. All metallic components in XPS spectra were fitted using a Doniach-Šunjić lineshape [47] and a Shirley background was subtracted in all cases. C and O lines were fitted, when needed, using a Lorentzian lineshape. More details on the analysis of XPS spectra can be found in the Electronic Supplementary Material.

REFERENCES

1. Astruc, D., Transition-Metal Nanoparticles in Catalysis: From Historical Background to the State-of-the Art. In *Nanoparticles and Catalysis*, Wiley-VCH Verlag GmbH & Co. KGaA: 2008; pp 1-48.
2. Sarkar, A.; Kerr, J. B.; Cairns, E. J., Electrochemical Oxygen Reduction Behavior of Selectively Deposited Platinum Atoms on Gold Nanoparticles. *Chemphyschem* **2013**, *14*, 2132-2142.
3. Desic, M.; Popovic, M. M.; Obradovic, M. D.; Vracar, L. M.; Grgur, B. N., Study of Gold-Platinum and Platinum-Gold Surface Modification and Its Influence on Hydrogen Evolution and Oxygen Reduction. *J Serb Chem Soc* **2005**, *70*, 231-242.
4. Ataee-Esfahani, H.; Wang, L.; Nemoto, Y.; Yamauchi, Y., Synthesis of Bimetallic Au@Pt Nanoparticles with Au Core and Nanostructured Pt Shell toward Highly Active Electrocatalysts. *Chem Mater* **2010**, *22*, 6310-6318.
5. Kowal, A.; Li, M.; Shao, M.; Sasaki, K.; Vukmirovic, M. B.; Zhang, J.; Marinkovic, N. S.; Liu, P.; Frenkel, A. I.; Adzic, R. R., Ternary Pt/Rh/Sno2 Electrocatalysts for Oxidizing Ethanol to Co2. *Nature Materials* **2009**, *8*, 325-330.
6. Kwon, Y.; Birdja, Y.; Spanos, I.; Rodriguez, P.; Koper, M. T. M., Highly Selective Electro-Oxidation of Glycerol to Dihydroxyacetone on Platinum in the Presence of Bismuth. *ACS Catalysis* **2012**, *2*, 759-764.
7. Wang, L.; Yamauchi, Y., Strategic Synthesis of Trimetallic Au@Pd@Pt Core−Shell Nanoparticles from Poly(Vinylpyrrolidone)-Based Aqueous Solution toward Highly Active Electrocatalysts. *Chem Mater* **2011**, *23*, 2457-2465.
8. Li, M.; Liu, P.; Adzic, R. R., Platinum Monolayer Electrocatalysts for Anodic Oxidation of Alcohols. *The Journal of Physical Chemistry Letters* **2012**, *3*, 3480-3485.
9. Xing, Y.; Cai, Y.; Vukmirovic, M. B.; Zhou, W.-P.; Karan, H.; Wang, J. X.; Adzic, R. R., Enhancing Oxygen Reduction Reaction Activity Via Pd−Au Alloy Sublayer Mediation of Pt Monolayer Electrocatalysts. *The Journal of Physical Chemistry Letters* **2010**, *1*, 3238-3242.
10. Prieto, M. J.; Tremiliosi-Filho, G., Surface Restructuring of Pt Films on Au Stepped Surfaces: Effects on Catalytic Behaviour. *Phys Chem Chem Phys* **2013**, *15*, 13184-13189.
11. Eyrich, M.; Diemant, T.; Hartmann, H.; Bansmann, J.; Behm, R. J., Interaction of Co with Structurally Well-Defined Monolayer Ptau/Pt(111) Surface Alloys. *The Journal of Physical Chemistry C* **2012**, *116*, 11154-11165.
12. Weststrate, C. J.; Lundgren, E.; Andersen, J. N.; Rienks, E. D. L.; Gluhoi, A. C.; Bakker, J. W.; Groot, I. M. N.; Nieuwenhuys, B. E., Co Adsorption on Au(310) and Au(321): 6-Fold Coordinated Gold Atoms. *Surf Sci* **2009**, *603*, 2152-2157.
13. Ruggiero, C.; Hollins, P., Interaction of Co Molecules with the Au(332) Surface. *Surf Sci* **1997**, *377-379*, 583-586.
14. Sandell, A.; Bennich, P.; Nilsson, A.; Hernnäs, B.; Björneholm, O.; Mårtensson, N., Chemisorption of Co on Cu(100), Ag(110) and Au(110). *Surf Sci* **1994**, *310*, 16-26.
15. Tereshchuk, P.; Freire, R. L. H.; Da Silva, J. L. F., The Role of the Co Adsorption on Pt Monolayers Supported on Flat and Stepped Au Surfaces: A Density Functional Investigation. *RSC Advances* **2014**, *4*, 9247-9254.
16. Prieto, M. J.; Carbonio, E. E.; Fatayer, S.; Landers, R.; de Siervo, A., Electronic and Structural Study of Pt-Modified Au Vicinal Surfaces: A Model System for Pt-Au Catalysts. *Phys Chem Chem Phys* **2014**.

17. Heimann, P.; van der Veen, J. F.; Eastman, D. E., Structure-Dependent Surface Core Level Shifts for the Au(111), (100), and (110) Surfaces. *Solid State Commun* **1981**, *38*, 595-598.
18. Powell, C. J.; Jablonski, A., Nist Electron Inelastic-Mean-Free-Path Database. National Institute of Standards and Technology: Gaithersburg, MD, 2010.
19. Yeh, J. J.; Lindau, I., Atomic Subshell Photoionization Cross Sections and Asymmetry Parameters: 1 [Less-Than-or-Equals, Slant] Z [Less-Than-or-Equals, Slant] 103. *Atomic Data and Nuclear Data Tables* **1985**, *32*, 1-155.
20. Mehmood, F.; Kara, A.; Rahman, T. S.; Henry, C. R., Comparative Study of Co Adsorption on Flat, Stepped, and Kinked Au Surfaces Using Density Functional Theory. *Phys Rev B* **2009**, *79*, 075422.
21. Meier, D. C.; Bukhtiyarov, V.; Goodman, D. W., Co Adsorption on Au(110)−(1 × 2): An Iras Investigation. *The Journal of Physical Chemistry B* **2003**, *107*, 12668-12671.
22. Michael Gottfried, J.; Christmann, K., Oxidation of Carbon Monoxide over Au(1 1 0)-(1 × 2). *Surf Sci* **2004**, *566-568*, 1112-1117.
23. Keister, J. W.; Rowe, J. E.; Kolodziej, J. J.; Madey, T. E. In *Photoemission Spectroscopy of Platinum Overlayers on Silicon Dioxide Films*, Salt Lake City, Utah (USA), AVS: Salt Lake City, Utah (USA), 2000; pp 2174-2178.
24. Hörnström, S. E.; Johansson, L.; Flodström, A.; Nyholm, R.; Schmidt-May, J., Surface and Bulk Core Level Binding Energy Shifts in Pt---Au Alloys. *Surf Sci* **1985**, *160*, 561-570.
25. Freire, R. L. H.; Kiejna, A.; Da Silva, J. L. F., Adsorption of Rh, Pd, Ir, and Pt on the Au(111) and Cu(111) Surfaces: A Density Functional Theory Investigation. *The Journal of Physical Chemistry C* **2014**, *118*, 19051-19061.
26. Stolbov, S.; Zuluaga, S., Factors Controlling the Reactivity of Catalytically Active Monolayers on Metal Substrates. *The Journal of Physical Chemistry Letters* **2013**, *4*, 1537-1540.
27. Bergbreiter, A.; Alves, O. B.; Hoster, H. E., Entropy Effects in Atom Distribution and Electrochemical Properties of Auxpt1−X/Pt(111) Surface Alloys. *Chemphyschem* **2010**, *11*, 1505-1512.
28. Ge, Q.; Song, C.; Wang, L., A Density Functional Theory Study of Co Adsorption on Pt-Au Nanoparticles. *Computational Materials Science* **2006**, *35*, 247-253.
29. 1995, *Handbook of X Ray Photoelectron Spectroscopy: A Reference Book of Standard Spectra for Identification and Interpretation of Xps Data*; Perkin-Elmer coorporation: USA, John F. Moulder, William F. Stickle, Peter E. Sobol, Kenneth D. Bomben.
30. Tao, F.; Dag, S.; Wang, L. W.; Liu, Z.; Butcher, D. R.; Bluhm, H.; Salmeron, M.; Somorjai, G. A., Break-up of Stepped Platinum Catalyst Surfaces by High Co Coverage. *Science* **2010**, *327*, 850-853.
31. Webb, M. J.; Palmgren, P.; Pal, P.; Karis, O.; Grennberg, H., A Simple Method to Produce Almost Perfect Graphene on Highly Oriented Pyrolytic Graphite. *Carbon* **2011**, *49*, 3242-3249.
32. Rebholz, M.; Prins, R.; Kruse, N., Adsorption and Dissociation of Co on Rh(210). *Surface Science Letters* **1991**, *259*, L797-L803.
33. Beutler, A.; Lundgren, E.; Nyholm, R.; Andersen, J. N.; Setlik, B.; Heskett, D., On the Adsorption Sites for Co on the Rh(111) Single Crystal Surface. *Surf Sci* **1997**, *371*, 381-389.
34. Matolin, V.; Rebholz, M.; Kruse, N., Defect-Induced Dissociation of Co on Palladium. *Surf Sci* **1991**, *245*, 233-243.
35. Alessandro, B., Structure and Chemical Reactivity of Transition Metal Surfaces as Probed by Synchrotron Radiation Core Level Photoelectron Spectroscopy. *Journal of Physics: Condensed Matter* **2008**, *20*, 093001.
36. Kinne, M.; Fuhrmann, T.; Zhu, J. F.; Whelan, C. M.; Denecke, R.; Steinrück, H.-P., Kinetics of the Co Oxidation Reaction on Pt(111) Studied by in Situ High-Resolution X-Ray Photoelectron Spectroscopy. *THE JOURNAL OF CHEMICAL PHYSICS* **2004**, *120*, 7113-7122.

37. McCrea, K.; Parker, J. S.; Chen, P.; Somorjai, G., Surface Structure Sensitivity of High-Pressure Co Dissociation on Pt(5 5 7), Pt(1 0 0) and Pt(1 1 1) Using Sum Frequency Generation Surface Vibrational Spectroscopy. *Surf Sci* **2001**, *494*, 238-250.
38. Tränkenschuh, B.; Fritsche, N.; Fuhrmann, T.; Papp, C.; Zhu, J. F.; Denecke, R.; Steinrück, H.-P., A Site-Selective in Situ Study of Co Adsorption and Desorption on Pt(355). *THE JOURNAL OF CHEMICAL PHYSICS* **2006**, *124*, 074712.
39. Ruban, A. V.; Skriver, H. L.; Nørskov, J. K., Surface Segregation Energies in Transition-Metal Alloys. *Phys Rev B* **1999**, *59*, 15990-16000.
40. Gottfried, J. M. Co Oxidation over Gold: Adsorption and Reation of Oxygen, Carbon Monoxide and Carbon Dioxide on Au(100)-(1x2) Surface Freien Universität Berlin, 2003.
41. Gottfried, J. M.; Schmidt, K. J.; Schroeder, S. L. M.; Christmann, K., Spontaneous and Electron-Induced Adsorption of Oxygen on Au(1 1 0)-(1×2). *Surf Sci* **2002**, *511*, 65-82.
42. Klyushin, A. Y.; Rocha, T. C.; Havecker, M.; Knop-Gericke, A.; Schlogl, R., A near Ambient Pressure Xps Study of Au Oxidation. *Phys Chem Chem Phys* **2014**, *16*, 7881-6.
43. Weinert, M.; Watson, R. E., Core-Level Shifts in Bulk Alloys and Surface Adlayers. *Phys Rev B* **1995**, *51*, 17168.
44. Brimaud, S.; Engstfeld, A. K.; Alves, O. B.; Behm, R. J., Structure–Reactivity Correlation in the Oxygen Reduction Reaction: Activity of Structurally Well Defined Auxpt1−X/Pt(111) Monolayer Surface Alloys. *J Electroanal Chem* **2014**, *716*, 71-79.
45. Brimaud, S.; Behm, R. J., Electrodeposition of a Pt Monolayer Film: Using Kinetic Limitations for Atomic Layer Epitaxy. *J Am Chem Soc* **2013**, *135*, 11716-11719.
46. Cezar, J. C., et al., The U11 Pgm Beam Line at the Brazilian National Synchrotron Light Laboratory. *Journal of Physics: Conference Series* **2013**, *425*, 072015.
47. Doniach, S.; Sunjic, M., Many-Electron Singularity in X-Ray Photoemission and X-Ray Line Spectra from Metals. *Journal of Physics C: Solid State Physics* **1970**, *3*, 285.